Imaging of primary retroperitoneal neoplasms

Ann. Ital. Chir., 2022 93, 5: 489-503
pii: S0003469X22038593

Emanuele Casciani*, Elisabetta Polettini*, Saadi Sollaku*, Gabriele Masselli*/**, Silvia Lanciotti*/**, Cristina De Angelis***, Gianfranco Gualdi*

**Reparto di Diagnostica per immagini, Clinica PIO XI, Roma, Italia*
***Radiologia DEA, Azienda Policlinico Umberto I, Roma, Italia*
****UOC Medicina Nucleare, Azienda Policlinico Umberto I, Roma, Italia*

Imaging of primary retroperitoneal neoplasms

Retroperitoneal soft tissue tumors are frequently incidental findings on imaging tests as Computed tomography (CT) or Magnetic Resonance Imaging (MRI). Retroperitoneal soft tissue tumors are rare and therefore not common in daily radiological practice. Clinician and radiologist'skills to set retroperitoneal soft tissue tumors at presentation is crucial for a correct patient management. So far, several diagnostic algorithms have been proposed to assess retroperitoneal masses, which have not been validated by case histories (2-5). The aim of this article is to evaluate a new classification of retroperitoneal masses using CT and MRI.

KEY WORDS: CT, Diagnosis, MRI, Retroperitoneum, Soft tissue sarcoma

Introduction

Retroperitoneal soft tissue tumors are frequently incidental findings on imaging tests such as Computed tomography (CT) or Magnetic Resonance Imaging (MRI) performed for other symptoms or diseases. Retroperitoneal soft tissue tumors are rare and therefore not common in daily radiological practice. Clinician and radiologist'skills to set retroperitoneal soft tissue tumors at presentation are crucial for a correct patient management. The long-term survival depends, after tumor biology, on the completeness of surgical resection; incomplete resections or contamination of the patient's peritoneal cavity could lead to catastrophic consequences due to poor expertise. Therefore, these patients should be referred to dedicated centers with a multidisciplinary team. Moreover, radiotherapy and chemotherapy appear to have a "new" adjuvant role [1].

Contrast-enhanced CT is the main imaging modality in retroperitoneal soft tissue tumors. CT is useful for masses localication, and primarily to distinguish between peritoneal and retroperitoneal masses. Tissue compositions (ie, lipomatous, cystic, calcifications, or myxoid) can also be evaluated by CT. MRI and CT have proven equally sensitive to the presence of disease with a few exceptions. MRI is a multiparametric tool with greater efficiency than CT for soft tissue characterization, and it is essential to assess pelvic masses extent, especially in female pelvises. MRI can also assist when in doubt on muscles, bones, foramina, and neurovascular structures involvement. Although imaging findings can be nonspecific, familiarity with the most relevant radiologic features, in combination with clinical and epidemiologic information, can aid the radiologist in narrowing the differential diagnosis or, in some cases, provide a specific diagnosis [2]. So far, several diagnostic algorithms have been proposed to assess retroperitoneal masses, which have not been validated by case histories [2-5].

The aim of this article is to evaluate a new classification of retroperitoneal masses using CT and MRI.

Pervenuto in Redazione Giugno 2022. Acettato per la pubblicazione Luglio 2022
Correspondence to: Emanuele Casciani (e-mail: emanuelecasciani @gmail.com)

Materials and methods

Patients

Between 2015 - 2020, we retrospectively enrolled 155 consecutive patients diagnosed with retroperitoneal mass with CT and/or MRI. The patients had signs or symptoms leading to a mass discovered by imagining or in other cases, the mass had been discovered as accidental finding, since the testing has been done for other pathologies or nonspecific symptoms.

CT and MRI Techniques

The patients were tested with CT (CT Revolution, General Electric) and/or MRI 3T (Signa, Pioneer, General Electric). CT protocol included preliminary unenhanced scans followed by triphasic examination (arterial, portal-venous, and late phase), after an intravenous injection of 100-120 ml of iodinated contrast material. MRI protocol included axial T1-weighted sequence, axial, coronal and sagittal T2-weighted sequences, axial T2-weighted with fat saturation sequence, and axial and coronal T1-weighted sequences with fat saturation before and after intravenous contrast media.

Image Interpretation

The classification of the retroperitoneal masses is difficult because they are often bulky and heterogeneous at presentation. Based on the previously diagnostic algorithms [2-5], we proposed a new classification to set the masses that are most frequently found in the retroperitoneum, i.e. liposarcomas, leiomyosarcomas, neurogenic forms and cystic forms (Fig. 1). The retroperitoneal masses has been classified as follows: group 1) solid masses containing adipose tissue mainly to identify liposarcomas; group 2) solid masses without adipose tissue with close contact with venous vessels to identify leiomyosarcomas; group 3) solid masses that do not fall into groups 1 and 2, located in the paravertebral / presacral area with the signs typical of neurogenic tumors; group 4) cystic masses. The radiologists were additionally asked to supply a precise diagnostic hypothesis of every single mass when possible, having knowledge of age, sex, symptoms and reasons of imaging tests, but not of histological examination results.

Results

Of the 152 patients with retroperitoneal masses that reached our observation, 47 were excluded since we had no histological test and 46 patients because of the masses were secondary to other tumors. Of the 59 patients (30 women and 29 men, age range 14-88 years; median age 60 years) enrolled, 30 patients were studied with CT, 13 patients with MRI, 16 patients with both CT and MRI.

The histological result was obtained from the surgical samples in 41 patients and the biopsy in 18 patients. The histological form types included in the study were 22 liposarcomas, 1 lipoma, 1 angiomyolipoma of the renal capsule, 6 leiomyosarcomas (arising from inferior vena cava in 2 patients, superior mesenteric vein in 2 patients, right gonadic vein in 1 patient, and common right iliac vein in 1 patient), 1 epithelioid haemangioendotheioma of the inferior vena cava, 1 mixofibroma, 1 malignant rhabdoid tumor, 1 clear cell sarcoma, 1 hemangiopericytoma, 1 extrauterine endometrial stromal sarcoma, 10 neurogenic tumors (1 schwannoma, 2 neurofibromas, 2 ganglioneuromas, 1 malignant peripheral nerve sheath tumor, 4 paragangliomas), 2 rabdiomiosarcomas, 4 cystic lymphangiomas, 4 taligut cysts, 1 cystic teratoma, and 1 extraskeletal sarcoma.

Group 1. Heterogeneous masses with macroscopic fat: liposarcomas and possible differential diagnosis

Table I summarizes clinical and imaging findings of this group of patients, including the diagnostic hypothesis and histological results. All masses containing adipose tissue have been correctly interpreted: 20 as liposarcomas, 1 as lipoma, 1 as renal angiomyolipoma and 1 as dermoid cyst. Of the 22 liposarcomas, 20 (90 %) were correctly classified. One myxoid and 1 pleomorphic liposarcomas had no visible adipose component in diagnostic tests.

Well-differentiated liposarcomas appeared at CT and MRI as well-defined predominantly fat-containing lesions with thick septa or soft-tissue attenuating nodularity that could exhibit mild to marked enhancement after contrast material administration (Fig. 2).No necrotic or hemorrhage zones were detected in a mass context in any of our cases of well-differentiated liposarcomas.

Of the 22 liposarcomas undergoing histological test, 5 resulted well-differentiated liposarcomas, 10 dedifferentiated liposarcomas, 5 pleomorphic liposarcomas, and 2 myxoid liposarcomas. Diagnostic hypothesis were correct in 3 out of 5 well-differentiated liposarcomas, and in 10 out of 10 de-differentiate liposarcomas. De-differentiated liposarcomas showed a well-differentiated fatty mass associated with a focal dominant non-adipose component (bimorphic lesion), clearly identifiable in 6 of the 10 de-differentiated liposarcomas of our cases (Fig. 3). Moreover necrotic and/or hemorrhage zones were evident in 4 cases of de-differentiated liposarcomas. In two de-differentiated liposarcomas the adipose component was hardly perceptible and the MRI resulted superior to the CT for a correct identification (Fig. 4). Typical findings were not encountered to correctly define subtypes of pleomorphic liposarcomas (4 cases) and myxoid

Table I - *Clinical and imaging features of retroperitoneal solid masses with adipose tissue*

N°	Age	Sex	Main symptoms / Exam reason	Imaging exams	Mass size (cm)	Key radiologic features	Diagnostic hypothesis	Histology
1	67	F	Flank pain	CT	7	Fat-containing lesion without thick septa	Lipoma	Lipoma
2	79	F	abdominal pain/fullness	CT	9	Fat-containing lesion with thick septa, cystic and solid components attached to renal parenchyma	Kidney AML	AML renal capsule
3	41	M	Abdominal discomfort	CT, MRI	8	Fat-fluid levels and calcifications	Dermoid cyst	Dermoid cyst
4	58	F	Asymptomatic abdominal mass	CT, MRI	23	fat-containing lesion with thick septa and nodule with avid c.e.	Dedifferentiated liposarcoma	Well-differentiate liposarcoma
5	88	M	No symptoms; prostate cancer staging	CT	8,5	fat-containing lesion without thick septa and nodule or c.e.	Well-differentiate liposarcoma	Well-differentiate liposarcoma
6	57	F	No symptoms	CT	18	fat-containing lesion with thick septa	Well-differentiate liposarcoma	Well-differentiate liposarcoma
7	58	F	No symptoms	CT	3,5	fat-containing lesion with thick septa, cystic and solid components;	Well-differentiate liposarcoma	Well-differentiate liposarcoma
8	81	M	Lumbar pain; dysuria	CT	22	fat-containing lesion without thick septa and nodule or c.e.	Dedifferentiated liposarcoma	Well-differentiate liposarcoma
9	77	F	flank pain	CT	11	Bimorphic lesion	Dedifferentiated liposarcoma	Dedifferentiated liposarcoma
10	69	F	Abdominal mass	CT, MRI	21	Bimorphic lesion	Dedifferentiated liposarcoma	Dedifferentiated liposarcoma
11	73	M	Abdominal mass, pain RIF	CT	18	large mass, avid c.e., necrosis and hemorrhage, low fat	Dedifferentiated liposarcoma	Dedifferentiated liposarcoma
12	77	M	Abdominal mass, pain LIF	CT	15	large mass, avid c.e., necrosis and hemorrhage, low fat	Dedifferentiated liposarcoma	Dedifferentiated liposarcoma
13	58	M	No symptoms	CT	11	Bimorphic lesion	Dedifferentiated liposarcoma	Dedifferentiated liposarcoma
14	71	M	No symptoms	CT	16	Bimorphic lesion	Dedifferentiated liposarcoma	Dedifferentiated liposarcoma
15	61	F	Asymptomatic abdominal mass	CT	18	Bimorphic lesion, hemorrhage	Dedifferentiated liposarcoma	Dedifferentiated liposarcoma
16	65	F	Asymptomatic abdominal mass	CT	17	Bimorphic lesion, hemorrhage	Dedifferentiated liposarcoma	Dedifferentiated liposarcoma
17	81	M	Flank pain	CT, MRI	12	fat-containing lesion with thick septa, cystic and solid components	Dedifferentiated liposarcoma	Dedifferentiated liposarcoma
18	67	M	No symptoms; lung cancer staging	CT	7	fat-containing lesion and solid components	Dedifferentiated liposarcoma	Dedifferentiated liposarcoma
19	49	M	Abdominal mass	MRI	8	large well defined soft-tissue masses, with necrosis and hemorrhage	Liposarcoma	Pleomorphic liposarcoma
20	40	F	Abdominal mass, constipation	CT	18	large mass, avid c.e., necrosis, low fat	Liposarcoma	Pleomorphic liposarcoma
21	88	F	Pain RIF	CT, MRI	9	large mass, avid c.e., necrosis, low fat	Liposarcoma	Pleomorphic liposarcoma
22	51	M	Renal colic	CT	8	large well defined soft-tissue masses, with necrosis and avid c.e.	Liposarcoma	Pleomorphic liposarcoma
23	78	M	Abdominal mass, asthenia	MRI	9	Heterogeneous T2 high signal heterogeneous c.e	Liposarcoma	Mixoid liposarcoma

Legend: RIF: right iliac fossa; LIF: left iliac fossa; CT: Computed Tomography; MRI: Magnetic Resonance Imaging;c.e: contrast enhanced

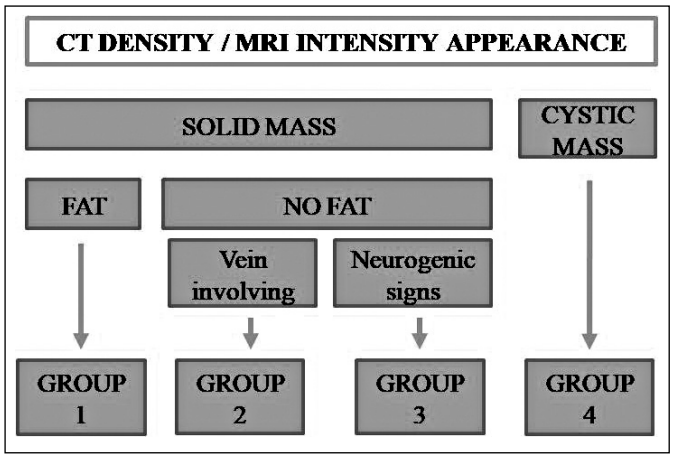

Fig. 1: Proposed diagnostic classification.

Fig. 2: Well-differentiated liposarcoma. Axial contrast-enhanced CT image shows a large heterogeneous well-defined predominantly fat-containing mass with thick septa (asterisk) and soft-tissue nodular components (arrow).

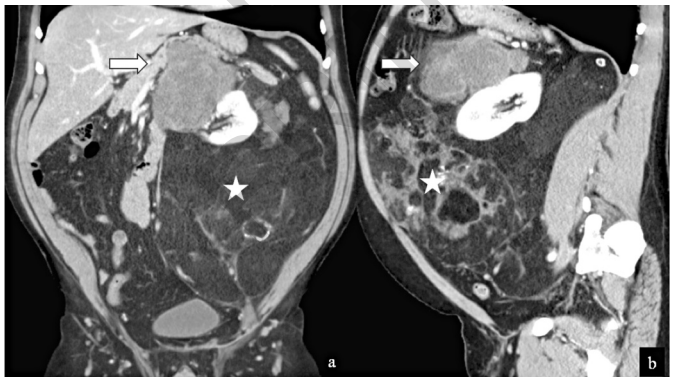

Fig. 3: Well and de-differentiated liposarcoma. Contrast-enhanced coronal (a) and sagittal (b) CT images show a large heterogeneous fat-containing mass (asterisk) with solid enhancing component between left kidney and pancreas (arrow), according to de-differentiation.

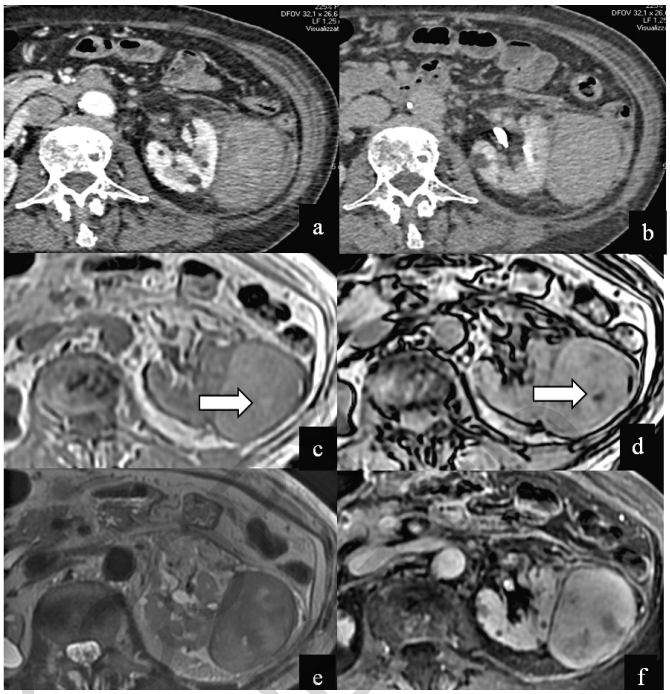

Fig. 4: De-differentiated liposarcoma. Axial portal phase (a) and delayed phase (b) contrast-enhanced CT images, axial in-phase (c) and out-phase (d) T1-weighted, axial T2-weighted (e), and contrast-enhanced axial T1-fat saturation (f) MRI images show left perirenal mass. In-phase (c) and out-phase (d) T1-weighted MRI images demonstrate fat content (arrows in c and d) that is invisible on CT, and in the other MRI sequences.

liposarcomas (3 cases) (Figs. 5, 6). In these subtypes however a scarce quantity or no evidence of adipose tissue, heterogeneous density/signal with hemorrhage and/or necrosis and avid contrast medium enhancement has been revealed. Finally, 3 masses with adipose tissue, without signs of liposarcoma, has been correctly interpreted as lipoma (Fig. 7), dermoid cyst (Fig. 8) and renal capsule angiomyolipoma (Fig. 9).

Group 2. Heterogeneous masses without fat and involving veins: leiomyosarcomas

Table II summarizes the clinical and imaging findings of this group of patients, including diagnostic hypothesis and histological results. All heterogeneous masses without adipose tissue and with close contact and / or involvement of veins have been correctly interpreted. Diagnostic hypothesis of leiomyosarcoma has been confirmed in 5 out of 8 cases (62 %), because the masses had an evident development along the interested vessels, that were superior mesenteric vein (two cases) (Fig. 10), inferior vena cava (two cases) (Fig. 11), and gonadic vein (Fig. 12). All cases had intravascular and extravascular components and internal necrosis. In the only case of our series in which an inferior vena cava mass was com-

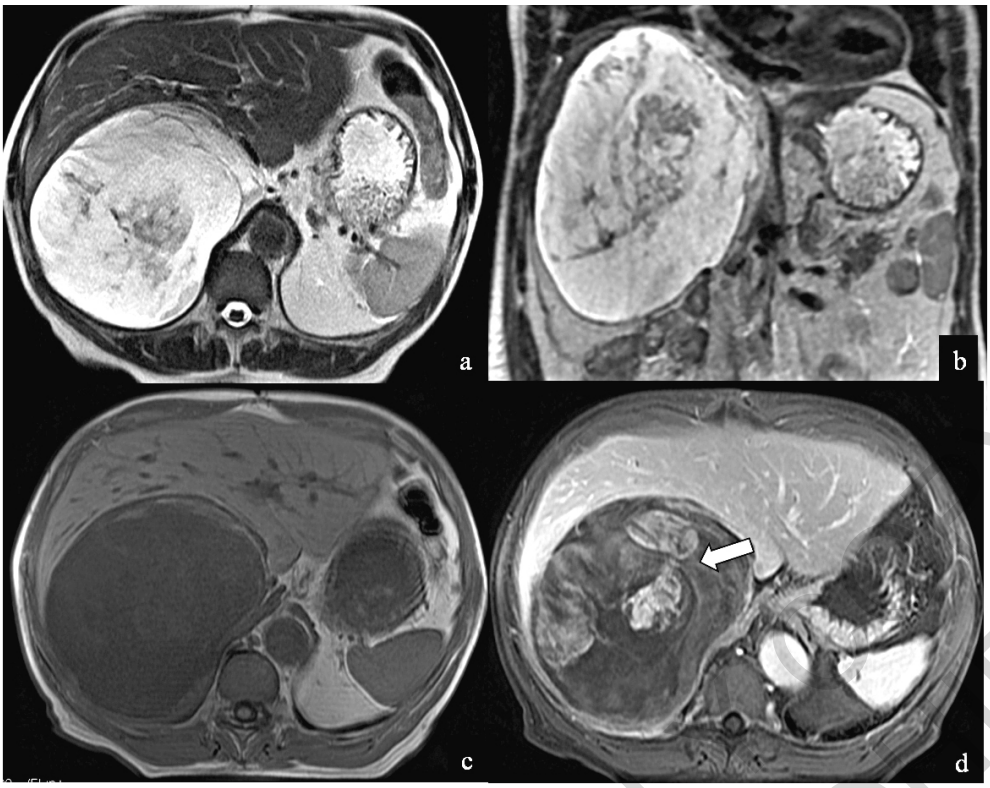

Fig. 5: Myxoid liposarcoma. Axial (a) and coronal (b) T2-weighted, axial T1-weighted (c), and axial contrast enhanced fat saturation T1-weighted MR images reveal right retroperitoneal encapsulated mass. The mass shows high signal intensity at T2-weighted and low signal intensity at T1-weighted due to the extracellular myxoid matrix, and patchy areas of enhancement at contrast enhanced fat saturation T1-weighted indicative of solid component (arrow).

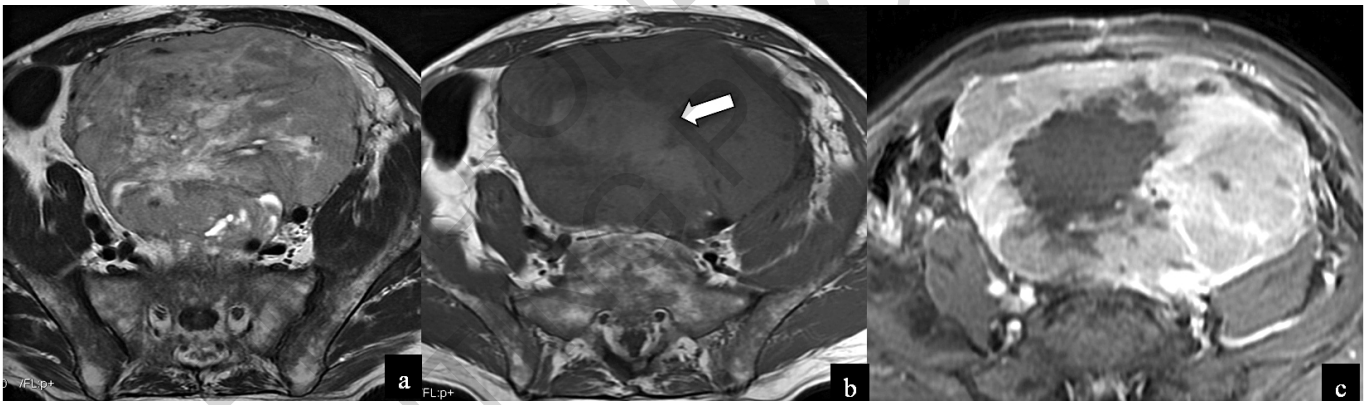

Fig. 6: Pleomorphic liposarcoma. Axial T2-weighted (a), T1-weighted (b), and axial contrast enhanced fat saturation T1-weighted (c) MR images show a large well defined retroperitoneal heterogeneous soft-tissue mass, with central areas of hemorrhage (arrow).

Fig. 7: Lipoma. Axial contrast-enhanced CT image shows a lipomatous mass occupying the retroperitoneal space into right iliac fossa without thick septa or soft-tissue nodular components (asterisk).

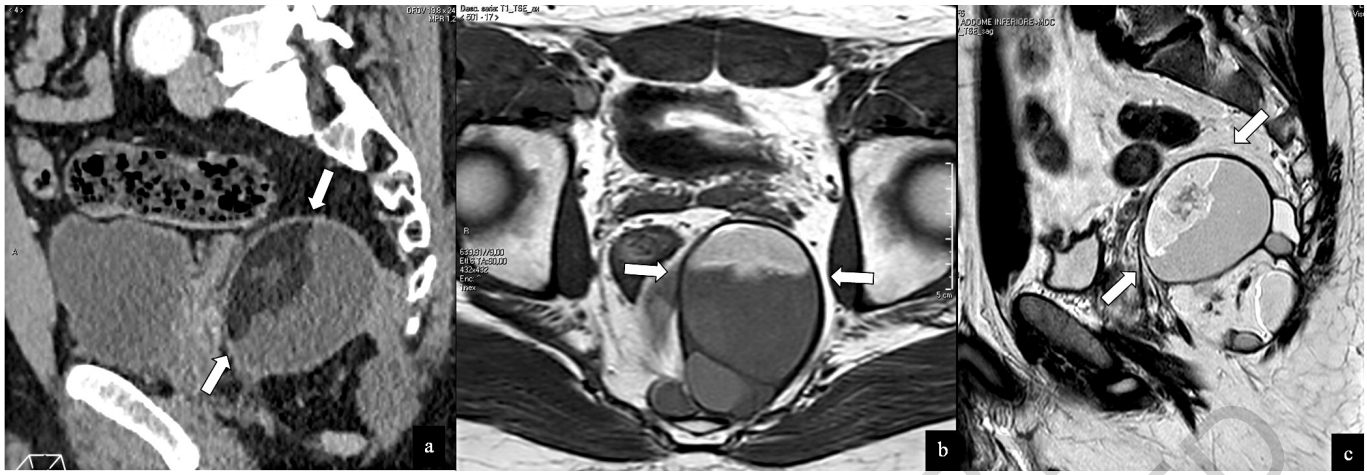

Fig. 8: Retroperitoneal mature cystic teratoma. Sagittal multiplanar reconstruction contrast-enhanced CT (a), axial T1-weighted (b), and sagittal T2-weighted (c) MRI images reveal a encapsulated mass in the presacral space with "fat-fluid level" (arrows), a typical sign of cystic teratoma.

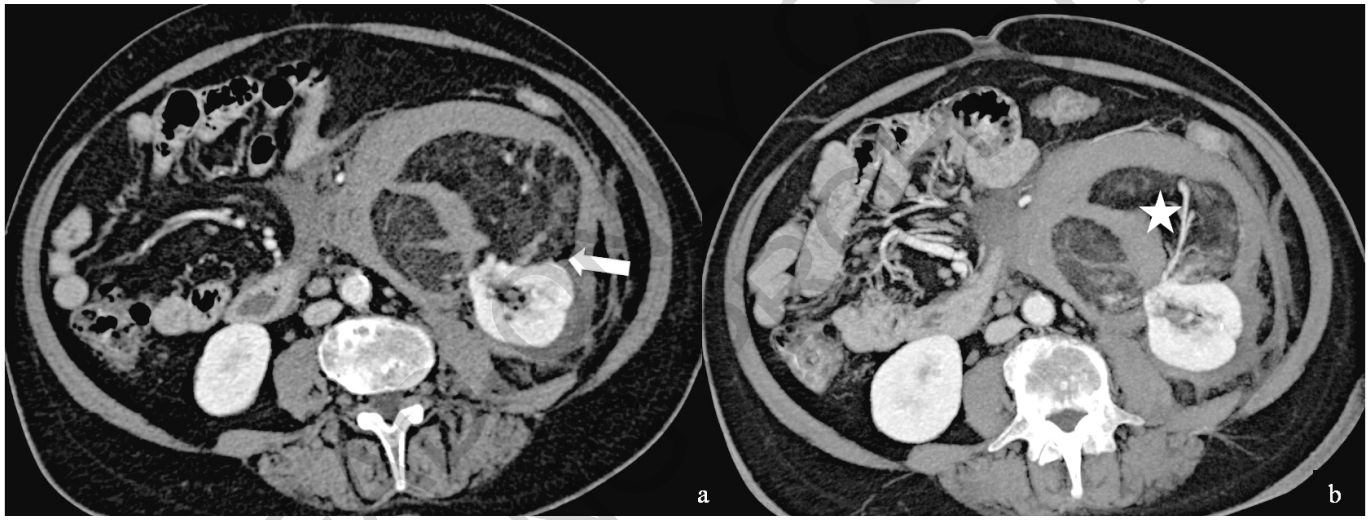

Fig. 9: Angiomyolipoma arising from renal capsule. Axial contrast-enhanced (a) and axial MIP (b)CT images show fat density retroperitoneal mass, associated with a left renal cortical defect (arrow) and prominent vessels (asterisk).

pletely intravascular, erroneously interpreted as leiomyosarcoma, the histological study demonstrated a rare case of primary epithelioid haemangioendotheioma (EHE) of the inferior vena cava (Fig. 13).
A leiomyosarcoma with a clear prevalence of the extravasal component was not included in this group. Voluminous size and unclear relation with to a venous vessel were the causes of the other two misinterpreted cases.

Group 3. Heterogeneous masses not eligible in groups 1 and 2, located in paravertebral / presacral space: neurogenic tumors

Table III summarizes the clinical and imaging findings of this group of patients, including diagnostic hypothesis and histological results. Of the 10 masses included in this group, 9(90 %) were correctly classified as neurogenic tumors. Radiologists have also mistakenly included an extraskeletal sarcoma in this group, which appeared to be a neurogenic tumor, because it was a paravertebral mass with intradural extramedullary component.
The typical imaging findings of the neurogenic tumors have been either the oval or hourglass morphology, the capsule shape, the paravertebral and the presacral site (Fig. 14), and the possibility to determine neural foramen enlargement (Fig. 15).
However, there was no finding to distinguish the different neurogenic forms from each other, apart from two cases of paraganglioma (Fig. 16), in which in addition to the radiological features there were also symptoms that could lead to the diagnosis, later confirmed by histological examination.

Table II - *Clinical and imaging features of retroperitoneal solid masses without adipose tissue with vein involvement: leiomyosarcoma*

N°	Age	Sex	Main symptoms / Exam reason	Imaging exams	Mass size (cm)	Key radiologic features	Diagnostic hypothesis	Histology
1	46	F	No symptoms	CT, MRI	2,5	Intravascular components, heterogeneous c.e	Intravascular leiomyosarcoma	EHE ICV
2	56	F	Pelvic pain	CT, MRI	10	Extravascular/ intravascular components, heterogeneous c.e, necrosis growing along the vessel	Leiomyosarcoma gonadic vein	Leiomyosarcoma gonadic vein
3	62	M	Pelvic pain	CT, MRI	8	Extravascular component, heterogeneous c.e, necrosis	Leiomyosarcoma iliac vein	Leiomyosarcoma iliac vein
4	49	F	Peripheral venous thrombosis	CT	13	Extravascular/ intravascular components, heterogeneous c.e, necrosis and hemorrhage	Leiomyosarcoma ICV	Leiomyosarcoma ICV
5	78	M	Lower extremity swelling	CT	11	Extravascular/ intravascular components; solid heterogenous c.e.; necrosis	Leiomyosarcoma ICV	Leiomyosarcoma ICV
6	75	F	Abdominal pain, mesenteric lymph-nodes at US	CT	20	Extravascular/ intravascular components; solid heterogenous c.e.; growing along the vessel	Leiomyosarcoma superior mesenteric vein	Leiomyosarcoma superior mesenteric vein

Legend: CT: Computed Tomography; MRI: Magnetic Resonance Imaging; c.e: contrast enhanced; EHE: epithelioid haemangioendotheioma; ICV: inferior cava vein

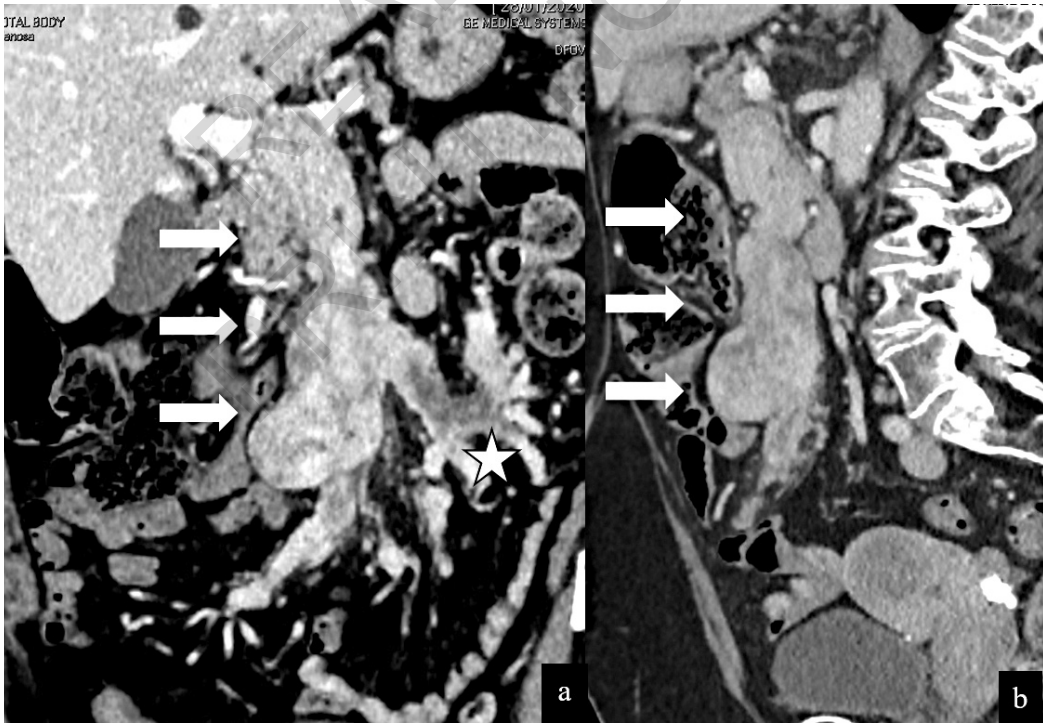

Fig. 10: Leiomyosarcoma of the superior mesenteric vein. Coronal (a) and MIP sagittal (b) contrast enhanced CT images reveal an heterogeneous mass developing along the superior mesenteric vein (arrows), causing thrombosis (asterisk).

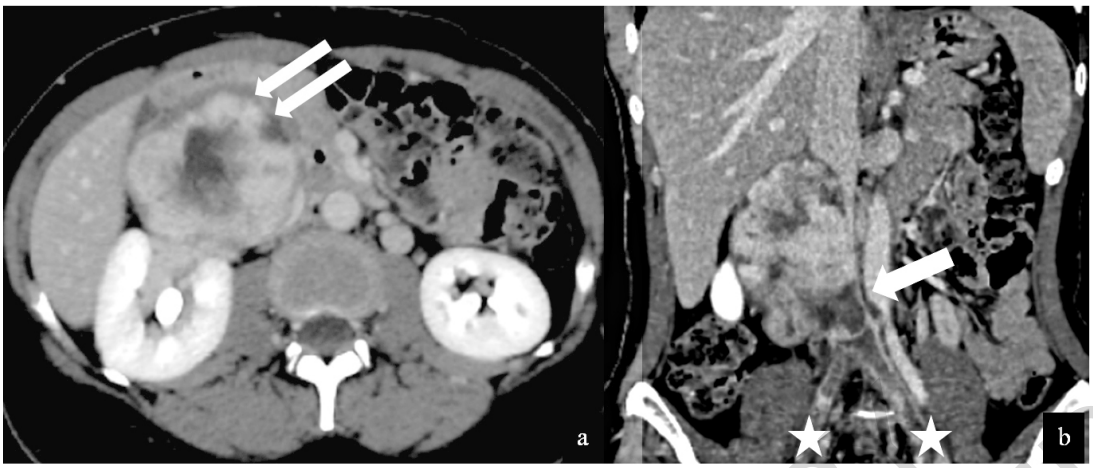

Fig. 11: Leiomyosarcoma of the inferior vena cava. Axial (a) and coronal (b) contrast enhanced CT images show a heterogeneous right perirenal mass consisting of exophytic component without invasion of the right kidney(arrows) and intraluminal component (arrow), resulting in iliac veins thrombosis (asterisks).

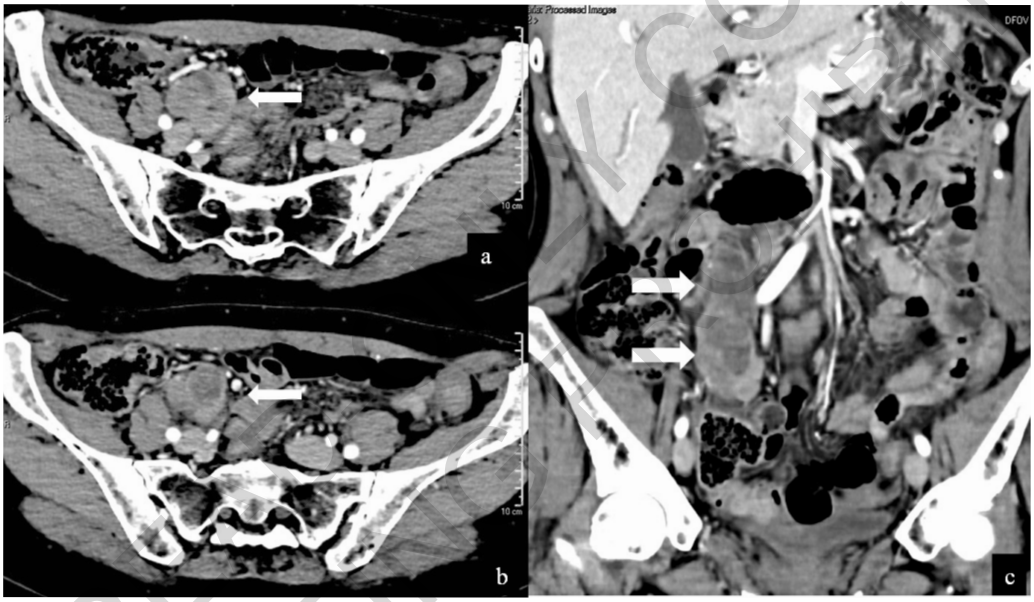

Fig. 12: Leiomyosarcoma of the gonadic vein. Axial (a and b) and MPR coronal (c) contrast enhanced CT images reveal an heterogeneous mass developing along the right gonadic vein (arrows).

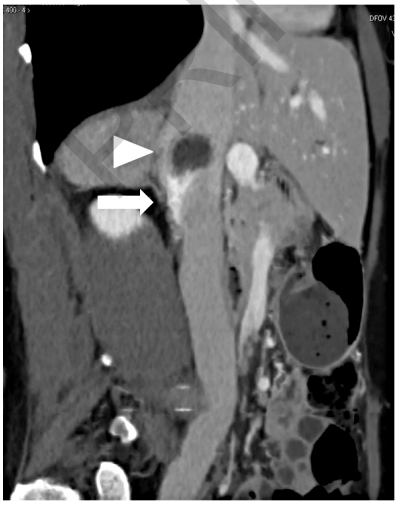

Fig. 13: Epithelioid haemangioendothelioma. Para-sagittal multiplanar reconstruction of venous phase of contrast enhanced CT shows an intraluminal non-enhancing mass (arrowhead) with peduncolated hypervascular structure (arrow) attached to the wall of the inferior cava vein.

Group 4. Cystic masses

Table IV summarizes clinical characteristics and imaging findings of this group of patients, including diagnostic hypothesis and histological results. Four cystic lymphangioma were classified correctly together with 4 tailgut cysts, while a completely cystic ganglioneuroma (Fig. 17) was mistakenly interpreted as cystic lymphangioma. A solid component indicative of malignant degeneration was evident in the context of one of tailgut's cysts (Fig. 18).

Our classification allowed to correctly categorize 80 % (47 out of 59) of retroperitoneal masses. Diagnostic hypothesis was correct in 32 of 59 cases (54 %). Table V summarizes the clinical and imaging findings of retroperitoneal masses that did not fall into the 4 categories proposed by our classification, including cystic ganglioneuroma that was erroneously included in group 4 and extremely rare neoplasms such as clear cell sarcoma, malignant rhabdoid tumor (Fig. 19), hemangiopericytoma (Fig. 20), extrauterine endometrial stromal sarcoma (Fig. 21), and urogenital rhabdomyosarcomas.

Discussion

A structured radiologic approach is necessary when a retroperitoneal mass needs to be evaluated. The proposed classification correctly classified 80 % of the retroperitoneal masses in our case series. However, our results confirm the difficulty to allocate retroperitoneal masses, which represents a very heterogeneous group of neoplasms. 12 out of 59 (20%) retroperitoneal masses did not fit into 1-4 groups planned in the proposed classification, including extremely rare neoplasms such as clear cell sarcoma [6], malignant rhabdoid tumor [7], hemangiopericytoma [8], endometrial stromal extrauterine sarcoma [9], and uro-genital rhabdomyosarcomas [10-12].

The accurate diagnostic hypothesis was correct in 54% of cases. This value may seem low, but the inclusion

Table III - *Clinical and imaging features of retroperitoneal solid masses not eligible for groups 1-2: neurogenic tumors*

N°	Age	Sex	Main symptoms / Exam reason	Imaging exams	Mass size (cm)	Key radiologic features	Diagnostic hypothesis	Histology
1	46	F	Adnexa mass at US	CT, MRI	7,5	Oval morphology, peripheral avid c.e. and central cystic degeneration	Neurogenic tumor	Neurogenic tumor (Schwannoma)
2	42	M	Lower back pain	MRI	9	Hourglass configuration; avid c.e.	Neurogenic tumor	Neurogenic tumor (Neurofibroma)
3	43	M	Chronic pelvic pain	MRI	9	Circumscribed oval mass, fascicular sign	Neurogenic tumor	Neurogenic tumor (Neurinoma)
4	50	M	Lower back pain	MRI	3	Well-defined mass, myxoid stroma, hypointense on T1-w, hyperintense on T2-w., slow progressive c.e.	Neurogenic tumor	Neurogenic tumor (Ganglioneuroma)
5	42	F	Lower back pain	MRI	9	Oval mass, mild c.e.	Neurogenic tumor	Neurogenic tumor (Ganglioneuroma)
6	67	M	LIF pain	CT	3	Solid mass with cystic component and calcifications	Neurogenic tumor	Neurogenic tumor (Malignant peripheral nerve sheath tumor)
7	53	F	Hypertension, tachycardia	MRI	6	circumscribed round mass hemorrhage; cystic component, no avid c.e.	Paraganglioma	Neurogenic tumor (Cystic praganglioma)
8	41	M	Hypertension, tachycardia	CT, MRI	4	Circumscribed round mass; cystic degeneration, calcifications; no avid c.e.	Paraganglioma	Neurogenic tumor (Paraganglioma)
9	68	F	No symptoms	CT	4.5	Polilobulate mass, homogeneous avid c.e; necrosis; "lightbulb" appearance	Neurogenic tumor	Neurogenic tumor (Paraganglioma)
10	15	M	Right lower back pain	CT, MRI	6	Paravertebral and intradural extramedullary, cystic degeneration, peripheral avid c.e, muscles involvement	Aggressive neurogenic tumor	Extraskeletal sarcoma

Legend: LIF: left iliac fossa; CT: Computed Tomography; MRI: Magnetic Resonance Imaging; c.e: contrast enhanced

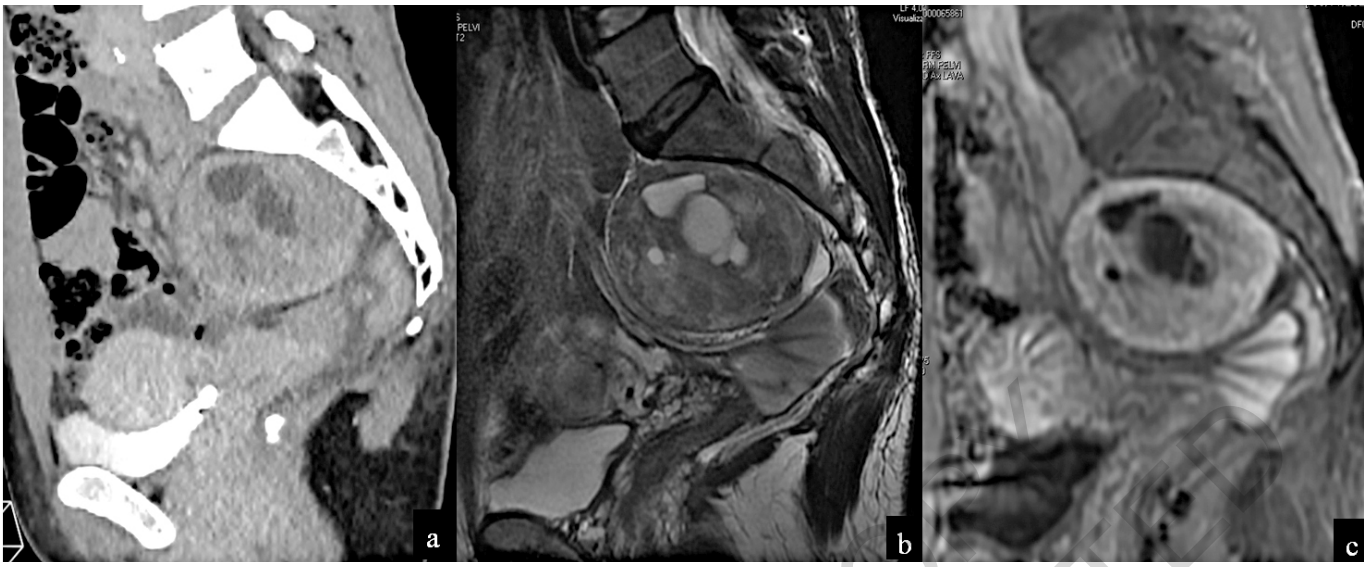

Fig. 14: Presacral schwannoma. Multiplanar reconstruction sagittal CT image (a), sagittal MRI T2-weighted image (b), and sagittal contrast-enhanced axial T1-fat saturation MRI image (c) show a solid mass with cystic components just anterior to sacrum, displacing rectum. Tumor contiguity to sacral nerve roots is not clearly visible.

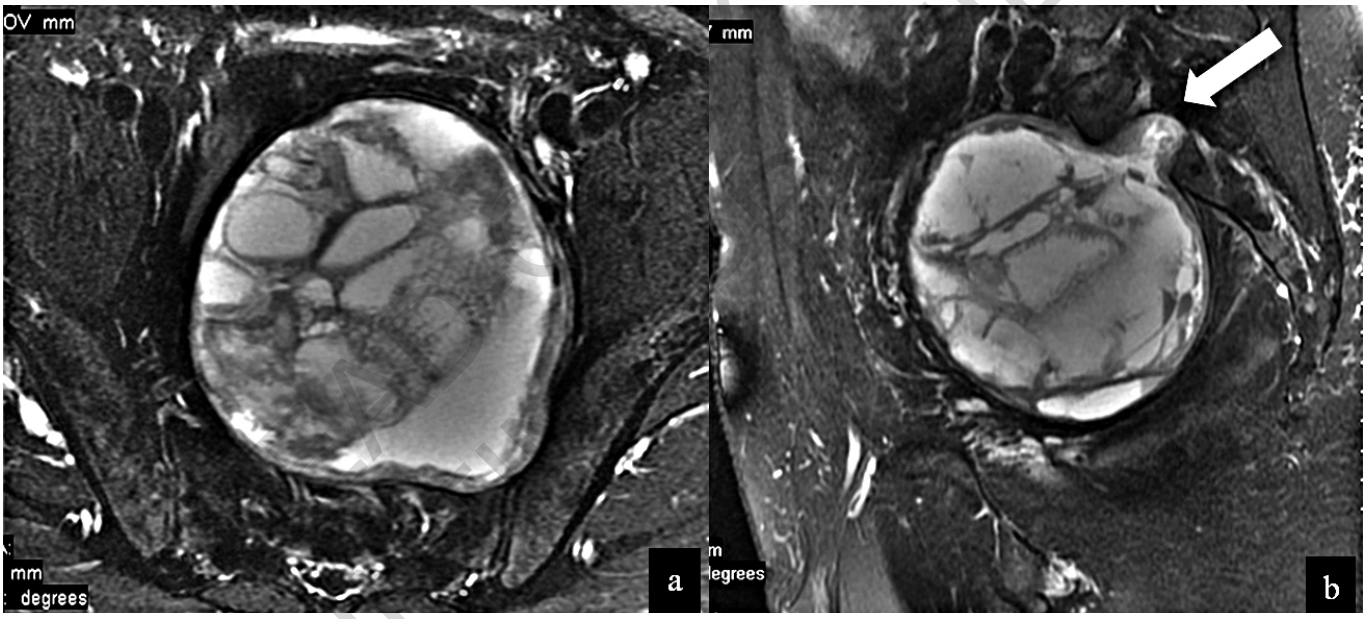

Fig. 15: Presacral schwannoma. Axial (a) and sagittal (b) T2-weighted fat saturation MR images show a huge well-defined heterogeneous solid lesion of mixed-signal intensity in the pelvis, arising from the sacrum with foraminal extension of the mass (arrow in b).

criteria chosen, such as liposarcoma subtypes, were very selective.

Liposarcomas are the most common primary retroperitoneal sarcomas, accounting for 37 % in our series and 35% of all malignant retropritoneal masses in literature [11]. Solid mass with macroscopic lipid is highly suggestive of liposarcoma [2]. In our study, 20 of 23 liposarcomas were correctly classified by the identification of adipose tissue in the context of the mass. Absence of macroscopic fat in a retroperitoneal mass does not exclude a diagnosis of retroperitoneal liposarcoma. This may represent disease that has dedifferentiated throughout or a sclerosing subtype. Moreover, myxoid and pleomorphic liposarcomas are often predominantly non-fatty (2), as found in our case studies, too. Histologically, retroperitoneal liposarcomas are classified into four subtypes: well-differentiated liposarcoma, de-differentiated liposarcoma, myxoid liposarcoma and pleomorphic liposarcoma. Well-differentiated and de-differentiated liposarcomas comprise the most common liposarcomas arising in the retroperitoneum, while myxoid and pleomorphic liposarcomas are rarely seen in the retroperitoneum [11,12], as our case history encountered (5/23 and 2/23, respectively).

TABLE IV - *Clinical and imaging features of retroperitoneal cystic masses*

N°	age	sex	Main symptoms / Exam reason	Imaging exams	Mass size (cm)	Key radiologic features	Diagnostic hypothesis	Histology
1	48	M	No symptoms	CT	6	Encapsulated cystic mass; no c.e.	Cystic lymphangioma	Cystic lymphangioma
2	43	F	No symptoms	CT	7	Encapsulated cystic mass; no c.e.	Cystic lymphangioma	Cystic lymphangioma
3	40	F	abdominal pain, fullness	CT	3	Encapsulated cystic mass; no c.e.	Cystic lymphangioma	Cystic lymphangioma
4	39	F	No symptoms	CT	6	Encapsulated cystic mass; no c.e.	Cystic lymphangioma	Cystic lymphangioma
5	57	F	Adnexa mass at US	MRI	4	Encapsulated presacral mass with high signal intensity on T1-w.	Tailgut cyst	Tailgut cyst
6	61	M	Pelvic pain	MRI	4	Encapsulated cystic mass with solid nodule; no c.e.	Tailgut cyst with malignant degeneration	Tailgut cyst with malignant degeneration
7	50	F	No symptoms	MRI	2,5	Encapsulated cystic mass with high signal intensity on T1-w; no c.e..	Tailgut cyst	Tailgut cyst
8	53	F	RIF pain	MRI	9	Encapsulated presacral mass with high signal intensity on T1-w.	Tailgut cyst	Tailgut cyst
9	76	M	Early satiety	CT	16	Encapsulated cystic mass; no c.e.	Cystic lymphangioma	Cystic ganglioneuroma

Legend: RIF: right iliac fossa; CT: Computed Tomography; MRI: Magnetic Resonance Imaging; c.e: contrast enhanced; US: ultrasound

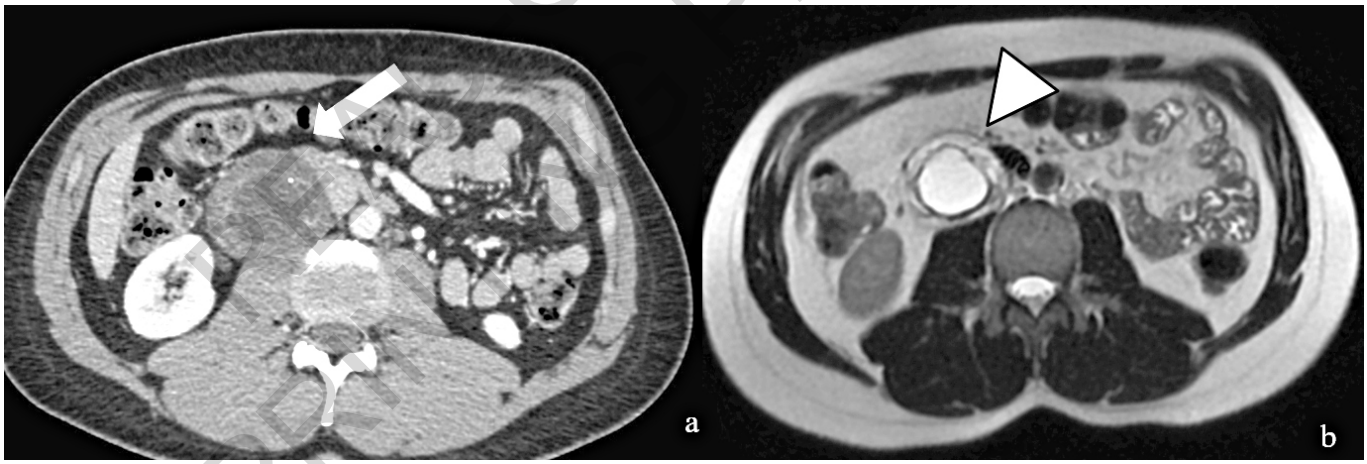

Fig. 16: Retroperitoneal paraganglioma with cystic degeneration. Axial contrast-enhanced CT image (a) shows a low-attenuation mass with tiny and curvilinear calcifications (arrow). Axial T2-weighted MR image (b) shows the mass to be heterogeneously hyperitense (arrowhead), with an internal cystic formation.

We have come across radiological signs that have often allowed correct classification of even well-differentiated liposarcoma subtypes and de-differentiated forms, whereas there are no radiological signs that have allowed distinction between myxoid and pleomorphic subtypes. Retroperitoneal lipomas are rare and may be indistinguishable from liposarcoma, and any retroperitoneal purely fatty lesion should be considered a well-differentiated liposarcoma rather than a lipoma until it is proven otherwise [2]. However, our lipoma case did not present septation nor wall thickening, neither increased density after contrast medium administration, and was therefore diagnosed as lipoma, later confirmed in bioptic examination.

Table V - *Clinical and imaging features of retroperitoneal solid masses not eligible into 1-4 groups*

N°	Age	Sex	Main symptoms / Exam reason	Imaging exams	Mass size (cm)	Key radiologic features	Diagnostic hypothesis	Histology
1	65	M	Abdominal mass, dysuria, constipation	MRI	15	Large mass, avid c.e., necrosis and hemorrhage (no fat)	Retroperitoneal mass	Pleomorphic liposarcoma
2	81	M	Abdominal mass	CT, MRI	17	Heterogenous solid, avid c.e. necrosis (no fat)	Retroperitoneal mass	Mixoid liposarcoma
3	50	F	Abdominal mass	CT, MRI	20	Heterogeneity hyperintensity T2-w. and c.e, calcifications, hemorrhage	Retroperitoneal mass	Leiomyosarcoma inferior cava vein
4	64	M	Abdominal pain	CT	6	Solid heterogenous c.e.; necrosis	Retroperitoneal mass	Leiomyosarcoma superior mesenteric vein
5	81	M	Abdominal mass	CT, MRI	15	Heterogeneity c.e. with necrosis, hemorrhage and calcifications	Retroperitoneal mass	Myxofibrosarcoma
6	67	M	Abdominal pain	CT	3	Heterogenous solid, avid c.e.;hemorrage	Retroperitoneal mass	Clear cell sarcoma
7	69	F	Lung cancer staging	CT	16	Heterogenous solid, avid c.e. necrosis	Retroperitoneal mass	Hemangiopericytoma
8	83	M	No symptoms	CT	5	Heterogenous solid, avid c.e. necrosis	Retroperitoneal mass	Extrarenal rhabdoid tumor
9	59	F	LIF pain	MRI	5	Heterogeneity hyperintensity T2-w. and c.e	Retroperitoneal mass	Endometrial stromal sarcoma extrauterine
10	14	F	Staging	CT, MRI	16	Solid heterogeneous mass with necrosis	Retroperitoneal mass	bladder RMS
11	50	F	Abdominal mass, pelvic pain	CT, MRI	18	Heterogeneity c.e. with necrosis, hemorrhage and calcifications	Retroperitoneal mass	bladder RMS
12	76	M	Early satiety	CT	16	Encapsulated cystic mass; no c.e.	Cystic lymphangioma	Cystic ganglioneuroma

Legend: LIF: left iliac fossa; CT: Computed Tomography; MRI: Magnetic Resonance Imaging; c.e: contrast enhanced; RMS: Rhabdomyosarcoma

Leiomyosarcomas are the second most common retroperitoneal sarcomas, accounting for 28% of all malignant retropritoneal masses in adult patients [12]. Leiomyosarcomas manifest as heterogeneous large masses arising from contiguous vessel (eg, the inferior vena cava) with extravascular component in 62% of cases, intravascular and extravascular components in 33% of cases [2], and only rarely, they are completely intravascular. In CT and MRI, heterogeneous contrast enhancement is usually found secondary to necrosis and hemorrhage. Calcifications are not commonly found, and adipose tissue is absent [2]. We correctly classified 5 out of 7 leiomyosarcomas encountered in our case studies, and the diagnostic hypothesis was histologicaly confirmed, thanks to the disposition of the vicinity or long vascular structure, as verified in the leiomyosarcomas arising from inferior vena cava, superior mesenteric vena and gonadic vena. Unfortunately, in some cases the prevalence of the extravasal component makes their diagnostic classification difficult, as we found in one of our cases. The bulky size of the mass may also mask its origin from a venous vessel.

The case of the primary EHE of the inferior vena cava was erroneously interpreted as completely intravascular leiomyosarcoma. Effectively intravascular neoplastic growth alone is possible, but it is extremely rare in leiomyosarcomas [12]. On the other hand, EHEs are extremely rare malignant tumors of vascular origin. Only few cases of this tumor, arising from inferior vena cava have been described in literature [13].

Fig. 17: Cystic ganglioneuroma. Axial (a) and coronal (b) contrast enhanced CT images show a encapsulated homogeneous hypodense mass, between inferior cava vein and aorta. It has cystic appearance ant it has been classified as cystic lymphangioma.

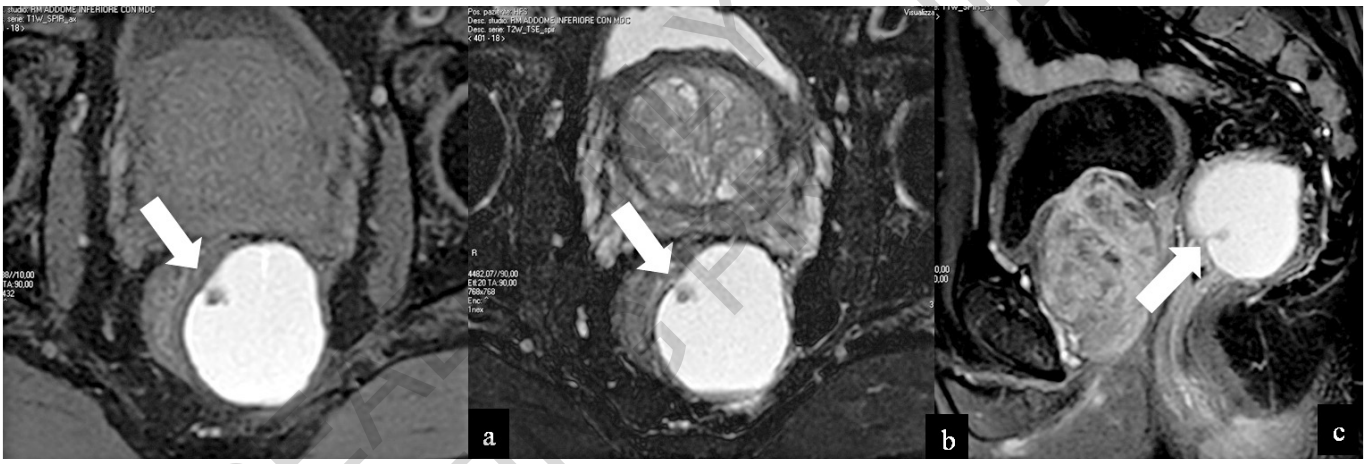

Fig. 18: Tailgut cyst with malignant transformation. Axial fat-suppressed T1-weighted (a), axial fat-suppressed T2-weighted (a) and sagittal fat-suppressed contrast-enhanced T1-weighted (c) MR images show a large cystic presacral mass with internal nodularity (arrows).

Fig. 19: Malignant rhabdoid tumor. Axial contrast-enhanced CT image shows retroperitoneal heterogeneous soft tissue mass with central necrosis and increased density after contrast medium administration (arrow).

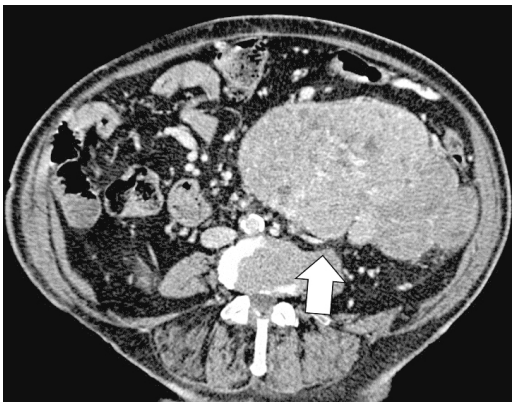

Fig. 20: Hemangiopericytoma. Axial contrast-enhanced CT image shows retroperitoneal heterogenous avid enhancement soft tissue mass (arrow).

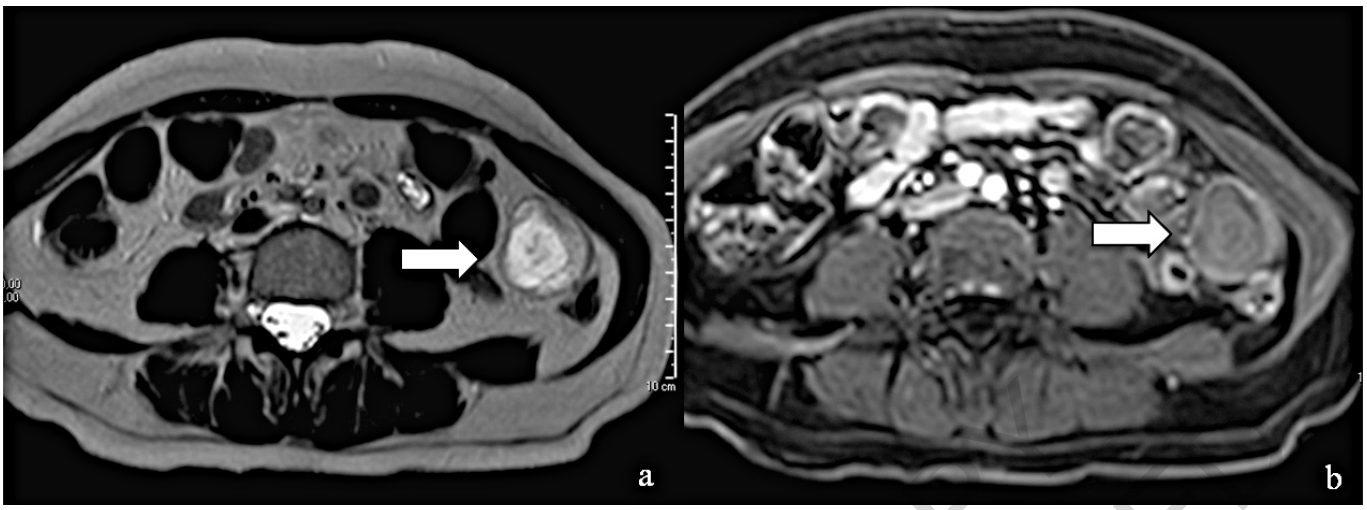

Fig. 21: Endometrial stromal sarcoma extrauterine. Axial T2-weighted (a) and axial contrast enhanced T1 fat saturation (b) reveal a heterogeneous encapsulate mass with high signal on T2-weighted and peripheral contrast enhancement on fat saturated T1-weighted (arrows).

Retroperitoneal neurogenic tumor commonly manifests radiologicaly as a well-defined, smooth or lobulated mass. Calcification may be seen in all types of neurogenic tumors. The diagnosis of retroperitoneal neurogenic tumor is suggested by the imaging appearance of the lesion, including its location, shape, and internal architecture [15-17]. Although all neurogenic tumors have similar clinical and radiologic findings, predominant or specific features can be present in each type [15]. However, in our patients, there was no peculiar feature to distinguish the different neurogenic forms from each other, apart from two cases of paraganglioma, in which in addition to the radiological features there were also symptoms that could lead to the diagnosis. Only one of the 10 neurogenous forms in our series was erroneously classified as cystic mass. It was a completely cystic ganglioneuroma that was interpreted as cystic lymphangioma. This possibility, although rare has already been described in literature [2,15].

Lastly, only 9 patients were enrolled with retoperitoneal cystic masses, which are quite uncommon with a reported incidence of only 1 in 100,000 adults [10]. This is also a heterogeneous group of lesions that include epithelial origin (eg, mucinous cystadenoma), mesothelial origin (eg, cystic mesothelioma), or germ cell origin (eg, cystic teratoma) [2]. Other lesions include tailgut cysts, cystic lymphangiomas, and epidermoid cysts. On rare occasions, schwannomas and paragangliomas can be completely cystic. In our series 4 cystic lymphangiomas, and 4 taligut cysts. Cystic lymphangiomas are characterized by thin-walled, unilocular or multilocular cystic mass, with variable attenuation depending on their content. Tailgut cysts are also more frequently identified in women and they appear as the other cystic entities mentioned above, but unlike the previous ones, they are always located in the presacral space. Malignant degeneration of tailgut cysts is much more frequent than previously believed [18], and radiological evidence of nodular thickening of the cyst wall significantly increased the relative risk of the presence of cancer, as detected in our case, too.

Conclusion

The proposed classification did not correctly categorize all primary retroperitoneal tumors that can be encountered in the retroperitoneum. In fact, retroperitoneal masses represent a very heterogeneous group of tumors that are difficult to classify, since radiological characteristics can also be similar and nonspecific in many cases. The knowledge of the distinctive radiological features together with the acquaintance of clinical considerations of retroperitoneal masses can help the radiologist to narrow the field of differential diagnoses and, in some cases, make a specific diagnosis.

The proposed classification for defining retroperitoneal masses needs further improvement for use in clinical practice.

Riassunto

Le masse retroperitoneali vengono scoperte molto frequentemente con le tecniche d'imaging (TC e RM) eseguite per altri motivi o per sintomi aspecifici. Le masse retroperitoneali sono rare e pertanto non sono frequenti nella pratica radiologica quotidiana.

La capacità del Clinico e del Radiologo di inquadrarle all'esordio è fondamentale per la corretta gestione del paziente. E' fondamentale che il paziente venga indirizzato in centri specializzati ove vi sia un approccio mul-

tidisciplinare, dal momento che, la sopravvivenza libera da malattia dipende, dopo la biologia del tumore, dalla radicalità del primo intervento chirurgico. Anche l'utilizzo di CHT e di RT prima o dopo l'intervento sono opzioni che necessitano di una valutazione multidisciplinare e possono fare la differenza nella sopravvivenza.
L'imaging ha molteplici ruoli nella valutazione delle masse retroperitoneali: individuare e stabilirne la sede, che non è scontata nelle forme voluminose; valutare il rapporto con le strutture vicine e l'infiltrazione di organi, visceri o vasi, fornendo elementi utili per il planning operatorio; valutare la multifocalità e la presenza di lesioni a distanza; guidare la biopsia della massa e ricercare un eventuale persistenza o recidiva di malattia nel follow-up. Un altro ruolo dell'imaging è quello di fornire elementi per la caratterizzazione.
Le caratteristiche radiologiche di questo gruppo eterogeneo di tumori possono essere simili. La conoscenza comunque delle caratteristiche specifiche all'imaging, unita alla conoscenza delle caratteristiche cliniche ed epidemiologiche delle masse retroperitoneali possono aiutare il radiologo a restringere il campo delle diagnosi differenziali e in alcuni casi fare una diagnosi specifica. Fino ad ora sono stati proposti diversi algoritmi diagnostici per inquadrare i tumori retroperitoneali basati sulla sede e sulle caratteristiche di densità in TC e di segnale in RM, ma non sono stati testati su casistiche.
Lo scopo di questo lavoro è stato quello di valutare l'attendibilità delle tecniche d'imaging di inquadrare i tumori retroperitoneali sulla base della classificazione che abbiamo proposto.

Ringraziamento

Questo articolo è stato realizzato con il contributo della Trade Art 2000 S.p.A.

References

1. Gronchi A, Miah AB, Dei Tos AP. et al: *Soft tissue and visceral sarcomas: ESMO-EURACAN-GENTURIS Clinical Practice Guidelines for diagnosis, treatment and follow-up.* Annal of Oncology 2021; 32: 1348-365.

2. Al-Dasuqi K, Irshaid L, Mathur M: *Radiologic-Pathologic Correlation of Primary Retroperitoneal Neoplasms.* Radio Graphics, 2020; 40:1631-657.

3. Messiou C, Morosi C: *Imaging in retroperitoneal soft tissue sarcoma.* J SurgOncol, 2018; 117:25–32.

4. Messiou C, Moskovic E,Vanel D, et al.: *Primary retroperitoneal soft tissue sarcoma: Imaging appearances, pitfalls and diagnostic algorithm.* EJSO 2017; 43: 1191-198.

5. MotaMMdS, Beserra ROF, Garcia MRT, et al: *Practical approach to primary retroperitoneal masses in adults.* Radiol Bras, 2018; 51: 391-400.

6. Katabuchi H, Honda T, Tajima T, et al: *Clear cell sarcoma arising in the retroperitoneum.* Int J Gynecol Cancer, 2002; 12:124-27.

7. Cai G, Zhu X, Xu Y, et al: *Case report of extrarenal rhabdoid tumor of pelvic retroperitoneum: Molecular profile of angiogenesis and its implication in new treatment strategy.* Cancer Biology & Therapy, 2009; 8:1-5.

8. Chhaidar A, Zouari S, Bdioui A, et al: *Very rare localization of a retroperitoneal hemangiopericytoma revealed by lumbosciatalgia: A case report.* Int J Surg Case Rep, 2018; 53: 127-31.

9. Giorgdaze T: *Retroperitoneal low grade endometrial stromal sarcoma with florid endometrioid glandular differentiation: Cytologic-histologic correlation and differential diagnosis.* Ann Diagn Pathol, 2019; 39:25-29.

10. Kransdorf MJ: *Malignant soft-tissue tumors in a large referral population: Distribution of diagnoses by age, sex, and location.* AJR Am J Roentgenol, 1995; 164:129-34.

11. Vijay A, Ram L: *Retroperitoneal Liposarcoma. A Comprehensive Review.* Am J Clin Oncol, 2015; 38:213-19.

12. Hartman DS, Hayes WS, Choyke PL, Tibbetts GP: *From the archives of the AFIP. Leiomyosarcoma of the retroperitoneum and inferior vena cava: Radiologic-pathologic correlation.* Radio Graphics, 1992; 12: 1203-220.

13. Gundara JS, Gill AJ, Neale M, et al: *Inferior vena cava epithelioid hemangioendothelioma.* J VascSurg: Venous and Lym Dis 2013; 1:75-7.

14. Dal Mo Y, Dong HJ, Hana K et al: *Retroperitoneal cystic masses: CT, clinical, and pathologic findings and literature review.* Radio Graphics, 2004; 24:1353-365.

15. Rha SE, Byun ZY, Zung SE, et al.: *Neurogenic tumors in the abdomen: Tumor types and imaging characteristics.* Radio Graphics, 2003; 23:29-43.

16. Clemente EJI, Navallas M, et al: *MRI of Rhabdomyosarcoma and Other Soft-Tissue Sarcomas in Children.* Radio Graphics, 2020; 40:791-814.

17. McCarville MB: *What MRI can tell us about neurogenic tumors and rhabdomyosarcoma.* Pediatr Radiol, 2016; 46:881-90.

18. Nicoll K, Bartrop C, Walsh S, et al.: *Malignant transformation of tailgut cysts is significantly higher than previously reported: Systematic review of cases in the literature.* Colorectal Dis, 2019; 21: 869-78.

19. Subramanian A, Maker VK: *Organs of Zuckerkandl: Their surgical significance and a review of a century of literature.* 2006; 192: 224-34.